Electrochemical studies on the oxidation of guanine and adenine at cyclodextrin modified electrodes

Abdolkarim Abbaspour* and Abolhassan Noori

Received 25th April 2008, Accepted 4th July 2008
First published as an Advance Article on the web 2nd September 2008
DOI: 10.1039/b806920d

An electrochemical sensor for guanine and adenine using cyclodextrin-modified poly(*N*-acetylaniline) (PNAANI) on a carbon paste electrode has been developed. The oxidation mechanism of guanine and adenine on the surface of the electrode was investigated by cyclic voltammetry. It was found that the electrode processes are irreversible, pH dependent, and involve several reaction products. The electron transfer process occurs in consecutive steps with the formation of a strongly adsorbed intermediate on the electrode surface. Also, a new method for estimating the apparent formation constants of guanine and adenine with the immobilized cyclodextrins, through the change of surface coverage of studied analytes has been reported. Both guanine and adenine showed linear concentrations in the range of 0.1–10 μM by using differential pulse voltammetry, with an experimental limit of detection down to 0.05 μM. Linear concentration ranges of 2–150 μM for guanine and 6–104 μM for adenine have been found when cyclic voltammetry was used for determination of both analytes.

1. Introduction

Investigations of the redox behavior of the biologically occurring compounds by means of electrochemical techniques have the potential for providing valuable insights into biological redox reactions of such biomolecules. Since the electroactivity of deoxyribonucleic acid (DNA) was discovered,[1] there have been intensive efforts to apply modern electrochemical methods in nucleic acid research and DNA analysis.[2] This is so because modern electrochemical techniques and related methodologies provide the most powerful approaches to elucidating mechanistic information concerning redox reactions.

Because guanine (**G**) is the most easily oxidized nitrogenous base, the chemical mechanism of its oxidation has been studied in detail.[3,4] While the mechanism of **G** and adenine (**A**) oxidation in solution has been well investigated, there have been very few mechanistic studies of the oxidation of these analytes at the surface of an electrode. This information would be useful for the design of electrochemical nucleic acid biosensors based on the detection of **G** and **A** oxidation.[5,6] In addition, previous solution electrochemistry studies have shown that uncatalyzed **G** and **A** electron transfer is slow at most electrode surfaces.[7]

The poor electron transfer kinetics from nucleic acids to most electrode materials has led many research groups to investigate the utility of having the detection of nucleic acids coupled to the detection of some second reporter molecule. Mikkelsen and coworkers detected DNA on carbon electrodes by immobilizing the DNA onto the electrode and then measuring the enhanced Faradaic current of $Co(bpy)_3^{2+/3+}$ in the presence of the surface attached DNA. In addition, numerous methods for attaching DNA to electrode materials have been described.[2,8–12] The electrochemical study of nucleic acids and their adsorption on different types of electrode materials has recently been of great interest.[13] These nucleobase oxidations have been observed when they are adsorbed onto carbon paste electrodes.[6] Wang *et al.* have focused on the detection of direct oxidation of the **G** and **A** bases adsorbed on carbon electrodes.[6,9,14,15] In addition, Kuhr *et al.* have achieved a sensitive detection system based upon catalytic oxidation of the deoxyribose (or ribose) sugar in nucleic acid at a copper microelectrode.[16,17] Our laboratory has also recently developed the use of chemically (mainly transition metal hexacyanoferrates as electrontransfer mediators) modified carbon paste electrodes for enhancing the voltammetric response of **G**, DNA and other biologically important analytes.[18]

Cyclodextrins (CDs) are oligosaccharides consisting of six, seven, or eight glucose units (named α, β, or γ-CD, respectively) which present a toroidal form with a hydrophobic inner cavity and a hydrophilic outer side.[19] Natural and chemically modified cyclodextrins can be viewed as molecular receptors. They can accommodate a wide variety of organic, inorganic, as well as biological guest molecules to form stable host–guest inclusion complexes or nanostructure supramolecular assemblies in their hydrophobic cavity, showing high molecular selectivity and enantioselectivity.[20]

Complexation abilities and analytical applications of working electrodes with attached cyclodextrins (CDs) have been reviewed.[21] CD and its derivatives modified electrodes have been prepared by Langmuir–Blodgett films of amphiphilic CD,[22] CD incorporated, carbon nanotubes-modified electrodes[23] and incorporating sulfonated CDs into polypyrrole.[24] Moreover, Kaifer *et al.* and Kitano *et al.* have reported self-assembled monolayers (SAMs) of thiolated CD and their derivatives, and have studied the association behavior of different analytes in the free state, and with surface-confined CDs.[25] Recently, Wu and Lin *et al.*[26] reported the preparation and characterization of a novel β-CD modified poly(*N*-acetylaniline) (CD/PNAANI) film.

Chemistry Department, College of Sciences, Shiraz University, Shiraz, 7145685464, Iran. E-mail: abbaspour@chem.susc.ac.ir; Fax: +98-711-2286008; Tel: +98-711-2284822

To our knowledge, there has been no report about the bonding properties of **G** and **A** on a surface confined CD electrode. The objective of this work was to study the oxidation mechanism of **G**, **A** and their oxidation products on a CD/PNAANI electrode in order to develop an electroanalytical procedure that could be applied to future determinations in biological fluids. For this purpose, cyclic voltammetry and differential pulse voltammetry were used.

2. Experimental

2.1. Apparatus

Voltammetric studies were accomplished using a Metrohm electroanalyzer (Model 757 VA Computrace). The three-electrode system consists of the bare or electrochemically modified carbon paste electrodes as the working electrode, Ag|AgCl|3M KCl as a reference electrode, and a Pt wire as a counter electrode in this system. The body of the working electrode was a Teflon cylinder (2.0 mm i.d.) that was tightly packed with carbon paste. A stainless steel rod inserted into the carbon paste established the electrical contact. A Metrohm 780 pH meter was used for pH measurements.

2.2. Materials

N-Acetylaniline (Merck) was used after recrystallization from ethanol. Lithum perchlorate, guanine, adenine, carbon powder and β-CD were obtained from Fluka. α-, and γ-CD were provided by TCI (Tokyo, Japan). All experiments were carried out at room temperature. Stock solutions of guanine and adenine (0.01 M) were prepared by dissolving appropriate amounts of analytes in diluted (0.2 M) NaOH solution followed by dilution with water to mark. The solutions were stored at 4 °C when not in use. Other chemicals were of analytical reagent grade and were used without further purification. Millipore deionized ultra pure water was used for preparing the solutions.

2.3. Poly(*N*-acetylaniline) film electrode

2.3.1. Fabrication of poly(*N*-acetylaniline) (PNAANI) film electrode. The required amount of mineral oil was mixed using a pestle with the needed amount of graphite (30–40% oil and 60–70% graphite was the optimum composition and between different oils, paraffin oil was the best, without any leakage, while, *e.g.* silicon oil was leaking during modification with CD in DMSO solution). A portion of the resulting paste was packed firmly into the cavity (2.0 mm diameter) of a Teflon tube. The PNAANI film electrode was prepared by electrodeposition of PNAANI in a 0.1 M *N*-acetylaniline, 1 M $HClO_4$ solution. The electrode potential at first was held at a constant voltage of 1.0 V *versus* Ag/AgCl for 1 min, and then swept from −0.20 V to 1.0 V for 20 cycles at a scan rate of 100 mV s^{-1}. In the process of electrolysis, an excellent cohesive brown film was formed on the electrode surface.

2.3.2. Fabrication of the CDs modified PNAANI electrode. The CDs modified PNAANI electrodes were fabricated by electrooxidation of the PNAANI electrodes in a DMSO solution of 0.05 M α-, β-, and γ-CD and 0.1M $LiClO_4$. The electrooxidation was carried out at a constant potential of 1.2 V for 10 min.

2.4. Procedure

Phosphate buffer (0.1 M, pH 7.0, 10 mL) was added into the electrochemical cell and the CD/PNAANI/CPE was activated by means of cyclic voltammetric sweeping from 0.2 to 1.2 V until the voltammograms were stable (~10 cycles). After that, the desired volume of standard **G**/**A** solution was added by micropipette. For the cyclic voltammetric determination, the preconcentration of the analyte at the CD-modified electrode was performed for a given period of time at the open circuit. During the pre-concentration time the solution was stirred by a magnet stirrer at about 100 rpm. Then cyclic voltammetries (CVs) were recorded in the same solutions (or in supporting electrolyte) using a scan rate of 100 mV s^{-1}. For repetitive measurements, the CD/PNAANI/CPE undergoes successive cyclic sweeping between 0.2 V to 1.2 V in the blank phosphate buffer (pH 7.0) to give a fresh electrode surface. An electrode surface prepared according to the mentioned procedure could be used at least for 5 independent analyses without need of PNAANI film regeneration.

The best parameters for differential pulse voltammetry (DPV) on the CD/PNAANI/CPE were accumulation time 120 s; pulse amplitude 0.05 V, scan rate 0.015 V s^{-1}, pulse time 0.04 s.

3. Results and discussion

3.1. Electrochemical behavior of the PNAANI film

The electrochemical formation of PNAANI film on CPE was performed by multicyclic voltammetry. Fig. 1 shows a typical cyclic voltammogram of deposition of the PNAANI film from a solution containing 0.10 M *N*-acetylaniline and 1.0 M $HClO_4$.

On successive scans, the peak currents increase slightly with each scan. This behavior indicates that a conductive polymeric film is coated onto the electrode. Three redox couples with E_0' of 190, 540, and 764 mV are observed. The characteristics of PNAANI film were the same as those deposited on GCE and discussed elsewhere.[26] In this paper our research is directed towards combining the advantageous features of carbon paste electrodes such as low background current and an easy surface

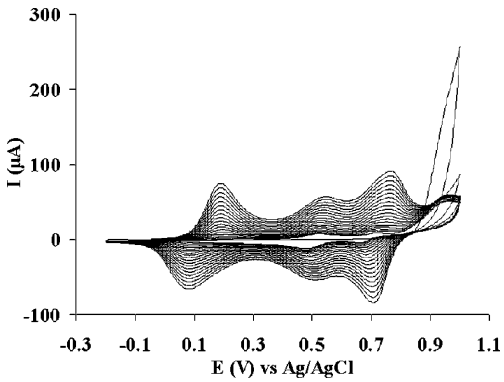

Fig. 1 Consecutive cyclic voltammograms of the growth of PNAANI film at the CPE in a solution containing 0.1 M *N*-acetylaniline in 1 M $HClO_4$. Scan rate: 100 mV s^{-1}.

renewability (of bare electrode) with PNAANI film. The first and third peaks, similar to polyaniline, are generally attributed to the oxidation of the base or protonated phenyleneamine units to the radical cation and their subsequent oxidation to the diradical dication, respectively.[27] The second peaks can be associated with the redox reaction of the degradation product containing the aromatic quinonoid group. The β-CD/PNAANI film has been characterized by X-ray photoelectron spectroscopy and ^{1}H NMR and the mechanism for β-CD incorporation into the polymer film has also been investigated.[25c] It is expected that incorporations of α- and γ-CD into the polymer film follow the same procedure.

To determine the electrooxidation time, when CD is incorporated into the PNAANI film saturately, the PNAANI electrode was electrooxidized for various times. I_{pa} increased gradually upon increasing the electrooxidation time (at 1.2 V in 0.05 M CD + 0.1 M $LiClO_4$/DMSO) and leveled off after 10 min. In addition, degradation studies on PNAANI film have shown that, it is unstable and quickly degradable under an applied potential of 1.2 V in acidic solution as well as chloride medium.[25e] For this reason, in this study the phosphate buffer pH 7.0 was chosen as the electrochemical reaction medium.

3.2. Electrochemical characteristics of guanine and adenine at CD/PNAANI/CPE electrode

In the present work, we examined the enhanced electrochemical responses of **G** and **A** at CD/PNAANI/CPE (taking β-CD as an example hereafter). Cyclic voltammograms of β-CD/PNAANI/CPE and bare carbon paste electrodes in the presence of **G** and **A** are shown in Fig. 2 (background currents are subtracted for simplicity).

At β-CD modified PNAANI carbon paste electrode, **G** and **A** exhibit anodic peaks at 0.74 and 0.97 V while similar peaks at a bare carbon paste electrode were obtained at 0.94 and 1.15 V, respectively. **G** and **A** exhibit no signal on the PNAANI modified electrode (PNAANI/CPE) in the absence of CD. Therefore, signals of **G** and **A** on CD/PNAANI/CPE are fully attributed to CD encapsulation effect. In addition, in the case of a bare carbon paste electrode, the voltammograms of **G** and **A** exhibit just a small hump peak. Compared to the electrochemical response on a bare electrode, at a β-CD modified electrode, the peak current signals of **G** and **A** enhance significantly and their oxidative potentials shifted negatively for about 200 mV and 180 mV for **G** and **A**, respectively. So, a CD modified electrode leads to the easier condition for their determination. No cathodic peaks were observed on the reverse scan within the investigated potential range which indicates that the oxidation of **G** and **A** are electrochemically irreversible processes. In order to perform the consecutive scan experiments on CD/PNAANI/CPE, firstly the solutions were mixed between consecutive runs and were allowed to stand for 120 s before starting the next scan. The results revealed that the current signals of **G** and **A** are very stable which indicates the rapid desorption of the reaction products. In the second experiment, the repetitive runs were just performed without mixing and standing. A sharp decrease (about 80%) of the peak currents were observed in the second scan and slow further current diminutions were observed in subsequent scans. Apparently, the modified electrode has an interfacial accumulation effect for **G** and **A**. Indeed, the adsorption/desorption properties of reagents and products and diffusion of the analytes are important influencing factors. Furthermore, these voltammetric responses were reproducible with a small electrode-to-electrode variation. It was found that the voltammetric response of the **G** and **A** obtained at the CD-modified electrode was stable and the electrode could be subjected to storage in distilled water for at least 3 days and for 5 independent analyses.

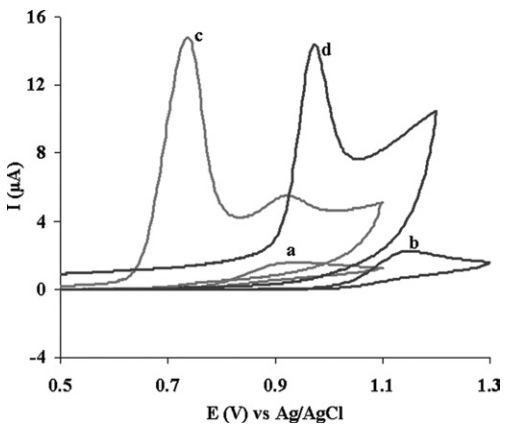

Fig. 2 CVs of bare (curves a and b) and CD-modified (curve c and d) electrodes in 0.1 M phosphate buffer related to **G** (curves a and c) and **A** (curves b and d). Scan rate, 100 mV s^{-1} (background currents are subtracted).

We examined the different inclusion behavior of three typical kinds of CDs. Compared with the electrochemical behavior on the β-CD modified electrode, the response signals of **G** and **A** on α-, and γ-CD modified electrodes were also considerable. Considering internal cavity diameters of α- (*ca.* 0.47–0.53 nm) and γ- (*ca.* 0.75–0.83 nm) compared with β-CD (*ca.* 0.60–0.66 nm),[28] it can be comprehended indirectly that in addition to inclusional complexation, some other interactions such as electrostatic bonding are taking part in purine-CD interactions. So, besides strong inclusional bondings, weak electrostatic bondings as well as nonbonding interactions exist in this system.[29]

The oxidation peak currents of **G** and **A** after 120 s of accumulation at different potentials were measured. The results revealed that the accumulation potential did not affect the oxidation peak currents, and therefore open-circuit accumulation was performed in this work. The influence of accumulation time on the oxidation peak currents at the CD/PNAANI modified CPE was also investigated. The oxidation peak currents increased remarkably within the first 120 s, and then continued slowly. This is due to the fact that the adsorption of **G** and **A** on the CD-modified electrode's surface becomes nearly saturated.

The peak potentials of both **G** and **A** depend on the pH of the solution, and shift negatively with increasing pH. The oxidation peak currents also depend on the pH of the phosphate buffer solution. The oxidation peak currents of **G** and **A** at the β-CD-modified electrode changed slightly over the pH range of 5.0 to 9.0. The oxidation peak potentials (E_p) varied with pH according to equations: $E_p = 1.102 - 0.056$ pH ($r = 0.998$) and $E_p = 1.538 - 0.055$ pH ($r = 0.986$) for **G** and **A**, respectively. The slopes of each fitted line is close to the theoretical value, −0.0591 V per pH unit, which suggests that the electrode reactions proceed by

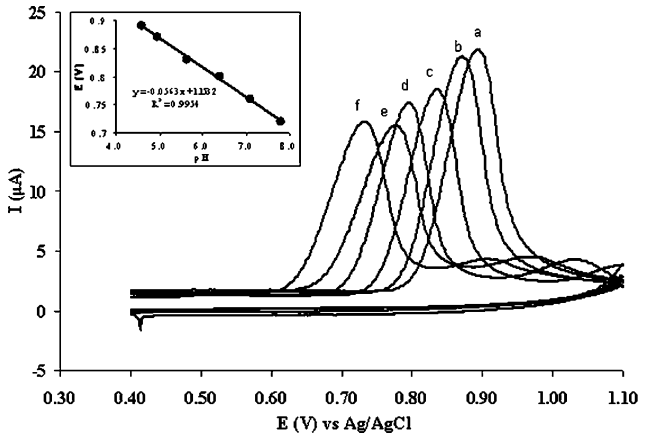

Fig. 3 Cyclic votammograms obtained in fixed concentration of the **G** as a function of pH: (a) 4.6, (b) 4.97, (c) 5.64, (d) 6.39, (e) 7.1, and (f) 7.78. Inset is the plot of anodic peak potentials (E_{pa}) *vs.* pH values.

a mechanism involving an equal number of electrons and protons. As an example, CVs and corresponding fitted lines for irreversible oxidation of **G** at different pHs are depicted in Fig. 3.

3.3. Determination of guanine and adenine

Two linear concentration ranges for **G** and **A** determination were observed using DPV and CV techniques. The first calibration curve for **G** (or **A**) in the presence of **A** (or **G**) in pH 7.0 phosphate buffer was obtained by DPV (Fig. 4). In this calibration curve the linear ranges after 120 s accumulation increased from 0.1 to 9.8 μM with the experimental limit of detection of 0.05 μM for both, and correlation coefficients of 0.998 and 0.995 for **G** and **A** respectively (Fig. 5).

In the second calibration curve of **G** and **A** determination, anodic peak currents of their oxidation from CVs were directly used. High concentrations from the second calibration curves (compared to first ones, obtained by using DPV) prevent simultaneous determination of both analytes. The oxidation

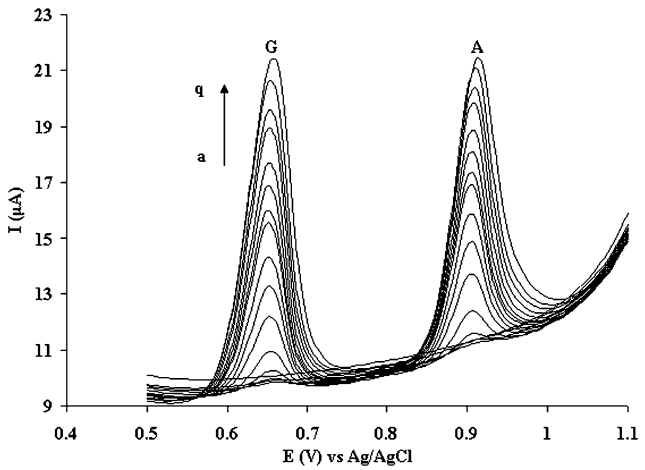

Fig. 4 DPVs for the **G** and **A** at β-CD/PNAANI/CPE in 0.1M phosphate buffer at pH 7.0 and different concentrations of analytes: (a) 0, (b) 0.1, (c) 0.2, (d) 0.5, (e) 1.0, (f) 2.0, (g) 4.0, (h) 6.0, (i) 7.9, (j) 9.8, (k) 11.7, (l) 14.6, (m) 17.5, (n) 21.3, (o) 25, (p) 29.8, (q) 34.5 μM. Accumulation time 120 s; pulse amplitude 0.05 V; voltage step 0.006 V; sweep rate 0.015 V s^{-1}.

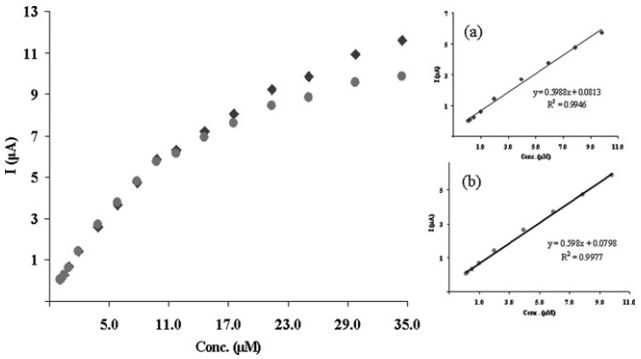

Fig. 5 Relationship between the increased oxidation peak current of **G** and **A** at CD-modified electrode and the concentration of **G** (●) and **A** (◆) corresponding to DPVs in Fig. 4; inset is the calibration curve of **A** (a) and **G** (b.).

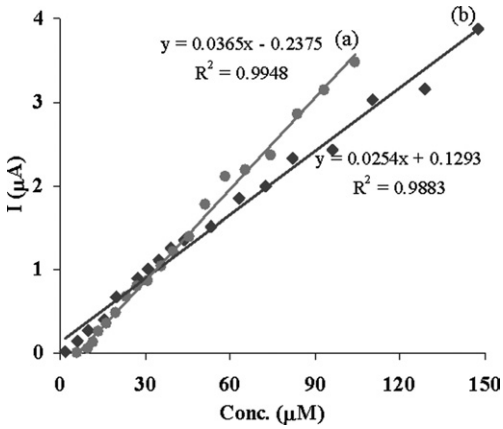

Fig. 6 Calibration curve based on anodic peak current of CVs for **A** (a) and **G** (b) at the β-CD-modified electrode in 0.1 M phosphate buffer pH 7.0.

peak of 2-oxo**A** (one of the oxidation products of **A**) interferes in **G** signal and oxidation of **G**'s oxidation products interfere in **A** oxidation current. This calibration curve lets us quantify the concentrations of **G** and **A** from 2–150 and 6–104 μM with experimental detection limits down to 1 μM level, respectively (Fig. 6). For achieving an extended dynamic range in the later case, CVs were recorded without any preconcentration times.

3.4. Adsorption isotherm for guanine and adenine inclusion

As inclusion into CD cavities is an equilibrium process, the number of cavities occupied is expected to vary with the concentration of guests in solution. The Langmuir isotherms have been used to determine the association constant (K_{ass}) in several CD monolayer systems.[30] In this study a scan rate of 100 mV s^{-1} was chosen to evaluate the **G** and **A** interactions with CD as this scan rate satisfactorily excludes solution phase interferences because peak currents are proportional to the root scan rate for solution-phase species but are directly proportional for surface bound species. Therefore, at high scan rates (>70 mV s^{-1}) the surface bound signal dominates the response. At higher scan rates (>100 mV s^{-1}), peaks were broadened and tend to featureless voltammograms.

The surface coverage (Γ) of **G** and **A** adsorbed onto the CD/PNAANI/CPE can be estimated from the coulometric charge obtained by integrating the anodic peak area in the cyclic voltammograms[31] and can be calculated out according to eqn (1):

$$\Gamma = Q/nFA \quad (1)$$

where Q is the amount of coulometric charge (C); n, the number of electrons transferred ($n = 2$); F, Faraday's constant, 96485 C mol^{-1}; A, the area of the unmodified electrode, 0.0412 cm^2. It is worthy to mention that the number of electrons transferred, correspond to oxidation of **G** to 8-oxo**G** (peaks a and b/c) and **A** to 2-oxo**A** (Fig. 9) for which the anodic peck area is considered.

Fig. 7(a) shows the dependence of surface coverage of **G** and **A** included into the cavity of CD as a function of bulk concentration of these analytes. Fig. 7(b) shows the linear form of the data according to eqn (3):

$$\frac{\Gamma}{\Gamma_{max} - \Gamma} = \beta C \quad (2)$$

$$\frac{C}{\Gamma} = \frac{C}{\Gamma_{max}} + \frac{1}{\beta \Gamma_{max}} \quad (3)$$

where Γ is the surface coverage in mol cm^{-2}, Γ_{max} is the saturation surface coverage and β is the apparent association constant for the guest-CD interaction, K_{ass} (M^{-1}).

Plots of C/Γ *vs.* C were linear and the good correlations of these plots indicate that the isotherms are a good model for the inclusion processes. The values found for K_{ass} and Γ_{max} are given in Table 1. Γ_{max} values are consistent with other reports of guest molecules included in CD monolayers.[32,28a] Nevertheless, some factors may introduce inaccuracies into the calculations of the surface coverages of **G** and **A**. The nonspecific bondings and disordered monolayer structure on the effective electrode areas in addition to adsorption of oxidation products might make the final attained data greater or smaller than the actual values.

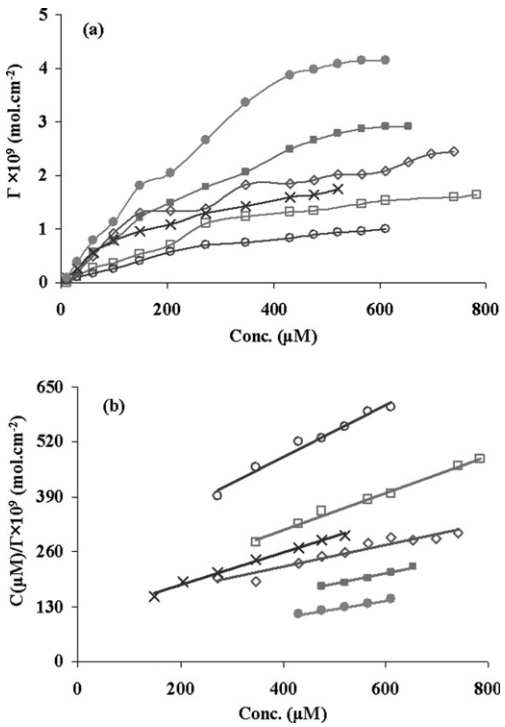

Fig. 7 (a) Measured **G** and **A** surface coverages on CDs/PNAANI/CPE electrodes as a function of the **G** and **A** concentrations at pH 7 of phosphate buffer solution; **A**-α-CD (–□–), **A**-β-CD (–○–), **A**-γ-CD (–◇–), **G**-α-CD (–■–), **G**-β-CD (–×–) and **G**-γ-CD (–●–). (b) C/Γ *vs.* C Langmuir plots of anodic peak current for the data of part (a) in which the symbols are the same.

Table 1 Maximum surface coverages (Γ_{max}) and the apparent association constants (K_{ass}) for the complexation of **A** and **G** with α-, β-, and γ-CD, confined at the PNAANI/CPE surface at an ambient temperature

	Guanine		Adenine	
	$K_{ass.} \pm$ SD/M^{-1}	$\Gamma_{max} \times 10^9$/ mol cm^{-2}	$K_{ass.} \pm$ SD/M^{-1}	$\Gamma_{max} \times 10^9$/ mol cm^{-2}
α-CD	4660 ± 273	3.91	3202 ± 341	2.28
β-CD	3630 ± 290	2.62	2576 ± 465	1.63
γ-CD	7724 ± 2038	5.07	2140 ± 168	3.87

3.5. Mechanistic investigation by cyclic voltammetry

Despite the sufficient peak separation of the studied analytes, we investigated them individually in order to not lose details of the mechanistic features. A variety of mechanistic pathways for oxidation of **G** and **A** in solution phase have been proposed and extensively reviewed in literature.[3,33] However, few of these mechanistic investigations have been reported for oxidation at the surface of the electrode.[34]

3.5.1. Mechanistic investigation of guanine. Cyclic voltammetry (CV) of **G** was carried out at the modified electrode in phosphate buffer pH 7.0. At this pH, **G** shows three oxidation peaks (a, b, and c) in its first scan. Representative CVs corresponding to mechanistic investigation of **G** oxidation at pH 7.0 and at different scan rates are shown in Fig. 8. CV (I) refers to oxidation of 0.5 mM **G** after 120 s accumulation time and recording the CV at the same solution. CV (II) was recorded at the same condition as (I) except that the electrode was transferred to the supporting electrolyte after 120 s accumulation time. With making a proper comparison between CVs (I) and (II), the net effect is a decrease in the height of the anodic peak current compared to that in the absence of diffusion (which is recorded in supporting electrolyte). This indicates that both adsorbed and diffusing analytes contribute to the current. In addition, at the very high scan rates, peak current (I_{pa}) approaches a proportionality with υ, while at low scan rates (up to 70 mV s^{-1}), I_{pa} approaches a better proportionality with $\upsilon^{1/2}$ which is characteristic of electrochemical behavior of absorbed reactant.[35]

At very slow sweep rates (5 mV s^{-1}) three oxidation peaks, a 0.7 V, b 0.82 V, and c 0.95 V, are monitored and oxidation peaks b and c are much smaller than peak a. Considering CV (I) and (II), it is obvious that peak a consists of two portions: first part, corresponds to those analyte molecules which are adsorbed at the electrode surface and make the inclusion complex with immobilized CD and the second portion is attributed to those analyte species which came to the electrode surface with diffusion

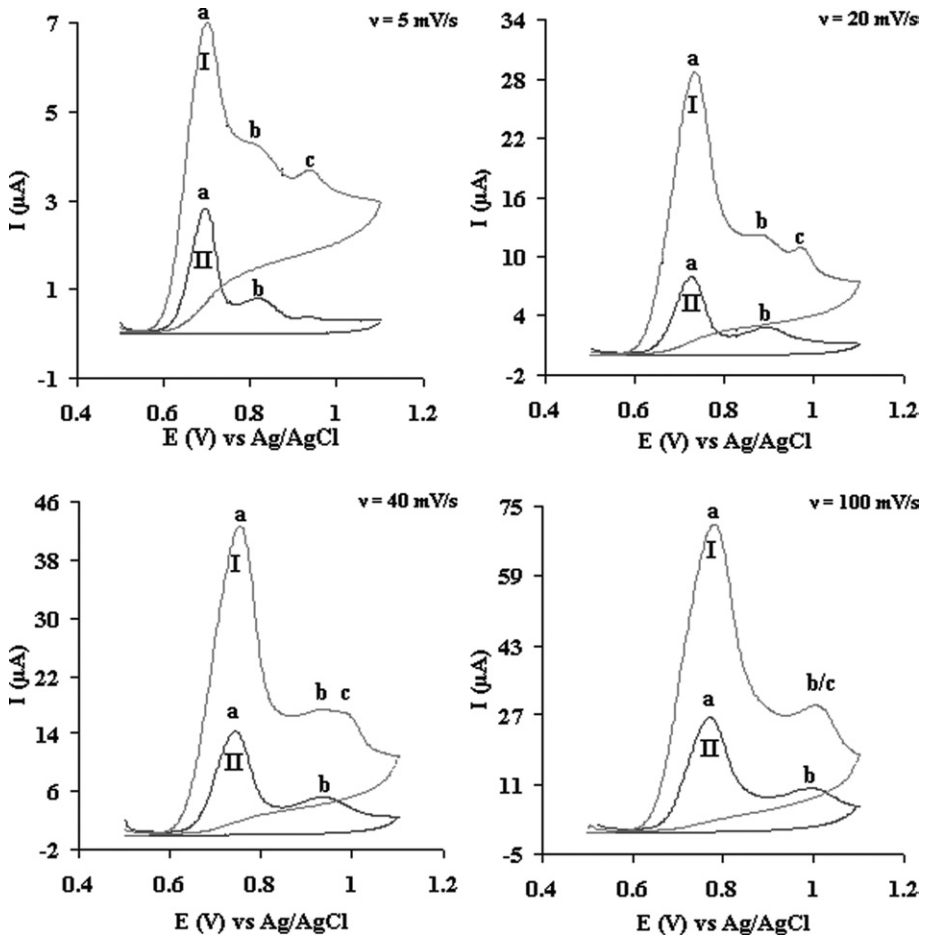

Fig. 8 CVs of **G** in 0.1 M phosphate buffer pH 7.0 recorded following its preconcentration onto a CD-modified electrode by adsorptive accumulation under open circuit conditions in different scan rates as denoted on them in a solution of 0.5 mM **G** (I) and after transferring the electrode to the buffer in the absence of **G** (II) (background currents are subtracted). All potentials are *vs.* Ag/AgCl reference electrode.

and oxidized on it. Oxidation peak b is one electron, irreversible oxidation process attributed to oxidation of $\mathbf{G}^{\bullet+}$ or **G**-dimmer[34] and takes place at more positive potentials than **G** itself. Oxidation peak c refers to those diffusing analytes which undergo oxidation reactions without specific bonding on surface-confined CD. So, diffusing analytes undergo an oxidation reaction by two different approaches. The major portions of diffusing species undergo oxidation at CD/PNAANI/CPE, with specific bonding to CD (a portion of peak a, Fig. 8), and the remaining oxidize at the CD/PNAANI/CPE electrode surface without any

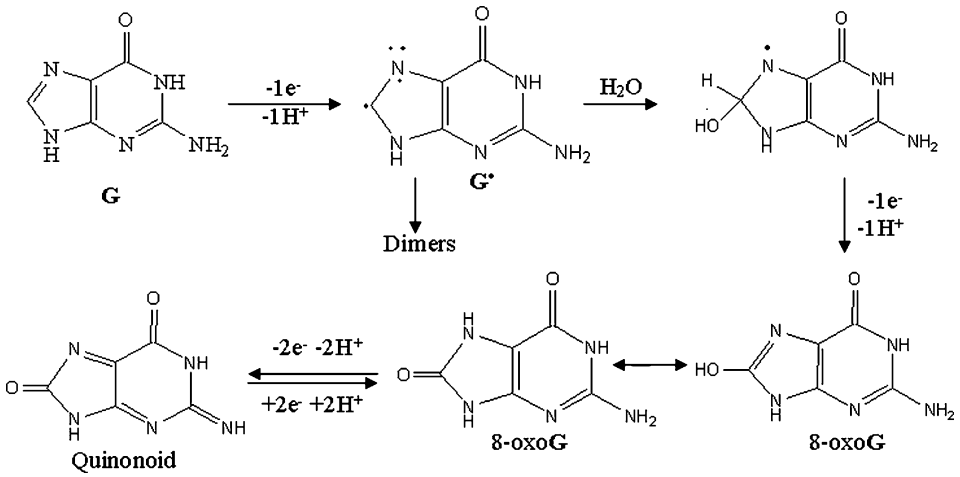

Scheme 1 General possible reaction mechanisms proposed for the oxidation of **G**.

specific interactions with the surface confined CD. Up to ν = 20 mV s^{-1} these three components of anodic peaks are distinguishable. With increasing sweep rate the height of peak a grows relative to that of c and shifts to more positive potentials. Thus, at a sweep rate of ≥60 mV s^{-1}, peaks b and c merge together (b/c). A positive shift of the anodic peak potential (a) with the increase of the scan rate indicates the slow kinetics of the interfacial electron transfer of **G**. The oxidation products of **G** diffusing away from the reaction sites and a dimerization reaction can occur as depicted in Scheme 1. Both of these effects cause the anodic peak potential of b to shift to more positive potentials (Fig. 8).

In order to determine the Tafel slope, the usual equation (eqn (4)) for a totally irreversible process[36] was employed:

$$E_p = (b/2) \log (\nu) + \text{constant} \quad (4)$$

where ν is the scan rate and b is the Tafel slope. A plot of E_p *vs.* log ν gave a linear relationship. The Tafel slope ($b = 0.059/\alpha n$) of 119 mV/decade was obtained, indicating one electron transfer is involved in the rate-determining step.

In addition, for a totally irreversible wave, E_p is a function of scan rate, shifting (for an oxidation) in a positive direction by an amount $1.15RT/\alpha nF$ (or $30/\alpha n$ mV at 25 °C) for each tenfold increase in ν.[35] E_p (corresponding to a) shifts 63 ± 5 mV more positive for every decade increase in sweep rate (5–50 mV s^{-1} or 10–100 mV s^{-1}). An approximate value of αn 0.46 was obtained, assuming α is equal to 0.46, the number of electrons in rate determining step is again one.

One reduction peak is observed in reverse sweep (Fig. 9(a)) and on the second anodic sweep, one new oxidation peak appears at less positive potentials than peak a. Reduction peak d appears to form a reversible couple with oxidation peak d' as is enlarged in the inset of Fig. 9(a). The cathodic and anodic peak currents were almost identical (both at 100 mV s^{-1}) and the peak-to-peak separation (ΔE_p) was *ca.* 28 mV, indicating that it is a 2 electrons reversible reaction corresponding to oxidation of 8-oxo**G** (Scheme 1).[37]

Investigation of the 3rd cycle at different scan rates (Fig. 10) revealed that at low scan rate (ν = 5 mV s^{-1}) oxidation products of **G** diffuse away and the peak current ratio of a to b is high. This ratio at a sufficiently high scan rate (ν = 200 mV s^{-1}) approaches unity since the diffusion of oxidation products are less probable. These observations indicate that peaks a and b belong to consecutive oxidations of one species in two steps.

3.5.2. Mechanistic investigation of adenine. Since the oxidation potential on CD/PNAANI/CPE is limited to 1.2 V, mechanistic investigation of **A** on this electrode encountered difficulties. Nevertheless, oxidation of **A** on a CD modified electrode shows about 180 mV shift compared to bare CPE

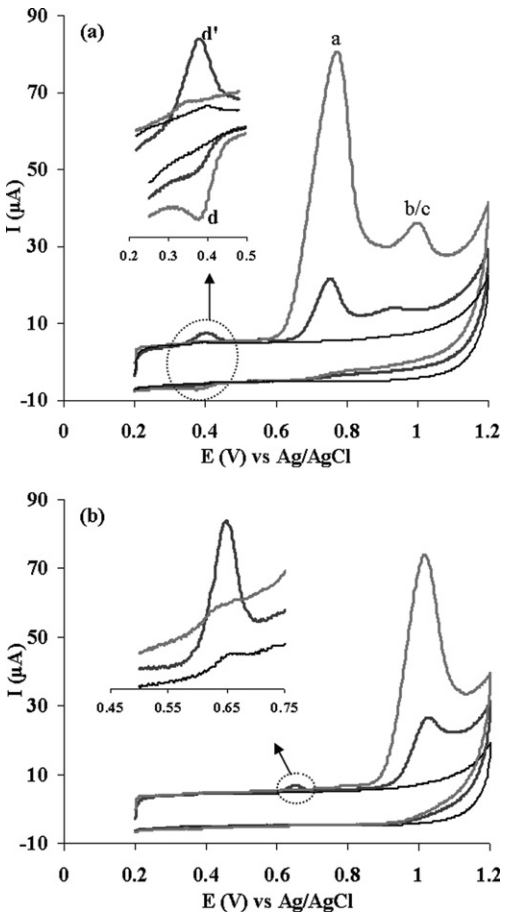

Fig. 9 First (light grey, red in HTML) and the second (dark grey, blue in HTML) CVs of 0.27 mM **G** (a) and **A** (b) in 0.1 M phosphate buffer. The responses between 0.25–0.5 (V) (a) and 0.5–0.75 (V) (b) have been scale-expanded in the inset. Preconcentration time; 300 s.

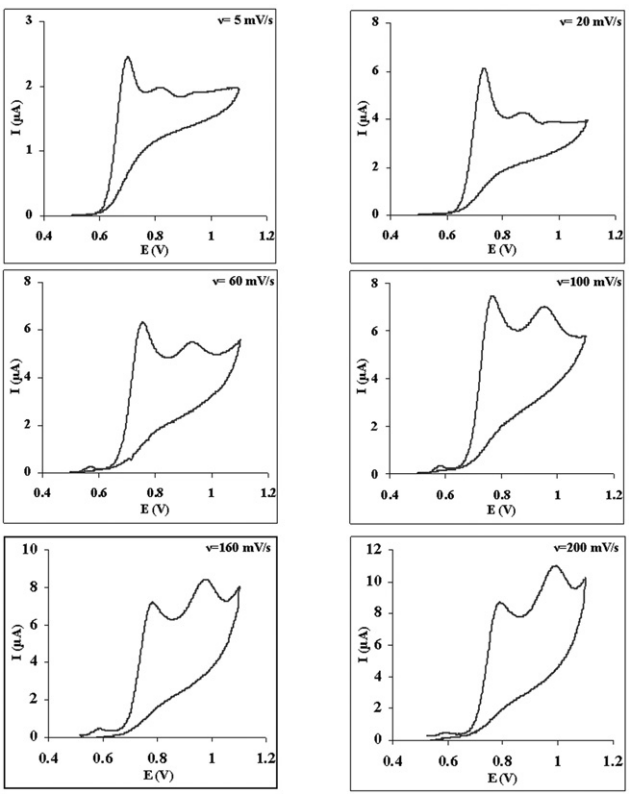

Fig. 10 CVs (3rd cycle) of 0.5 mM G recorded at different scan rates on β-CD-modified electrode (background currents are subtracted). All potentials are *vs.* Ag/AgCl reference electrode.

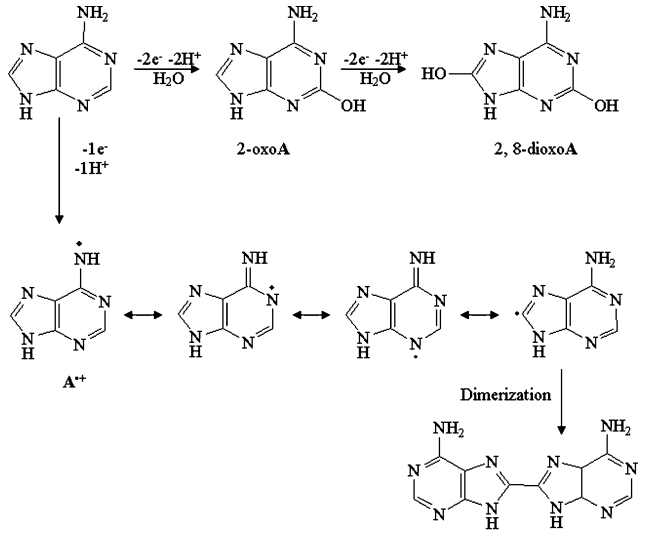

Scheme 2 General possible reaction mechanisms proposed for the oxidation of **A**.

which can be attributed to inclusional complexation of **A** with CD. Fig. 9(b) shows first and second voltammograms of **A** on a CD-modified electrode. In the first scan, one oxidation peak was observed which refers to the oxidation of **A** to 2-oxo**A**.[34] The electroactive **A** oxidation product, 2-oxo**A**, formed on the electrode surface was detected in the second cycle which undergoes an irreversible oxidation reaction. In this case, formation of dimmers is also possible which is reported in literature for **A** oxidation adsorbed on the electrode surface.[34]

The plot of E_p (corresponding to 2nd cycle) *vs.* log (v) is a straight line with a slope of *ca.* 59.2 mV. The Tafel slope b can be estimated as 104 mV according to eqn (4), which indicates that the number of transferred electrons involved in the rate determining step of the oxidation process is approximately one (n = 1). The same equation applied to the variation of log (v) *vs.* E_p of first cycle shows more deviation from the theoretical value (*i.e.* $n \approx 1.5$) which may be caused by oxidation of some other oxidation products (such as **A**-dimmer) at the same potential as **A**. Another possible mechanism for oxidation of **A** is its oxidation with two different pathways. In the first pathway, **A** undergoes a one electron oxidation reaction and leads to $\mathbf{A}^{\bullet+}$ and in the second path it is oxidized to 2-oxo**A** and consequently to 2,8-dioxo**A** (Scheme 2).

4. Conclusion

The CDs modified PNAANI film-coated CPE exhibits remarkable enhancement effects on the oxidation peak currents of **G** and **A**. Due to its strong adsorptive property as an inclusion complex, CD/PNAANI electrodes show very highly effective accumulation of **G** and **A**. These modified electrodes not only significantly improve the oxidation currents of **G** and **A**, but also negatively shift their oxidation potentials. Two calibration sets for both **G** and **A** were obtained. First linear concentration for both was in the range of 0.1–10 μM for using the DPV technique, and the second was from 2–150 and 6–104 μM for **G** and **A**, respectively, using the CV technique. Furthermore, in this paper, cyclic voltammetry was used to investigate the mechanism of **G** and **A** oxidations on CD-modified electrodes. These studies demonstrate that **G** and **A** can interact with CDs by both electrostatic interactions and supramolecular complexations. This study affords an effective method to investigate the interactions between analytes and their oxidation products with CDs, making use of surface-based electrochemical methods.

Finally, we have presented a new approach for using voltammetry in determining the binding constants of purines, as biologically important molecules, with CDs in a solvent system of 100% water.

Acknowledgements

We gratefully acknowledge the support of Shiraz University Research Council for this study.

References

1 E. Palecek, *Nature*, 1960, **188**, 656–657.
2 E. Palecek, *Electroanalysis*, 1996, **8**, 7–14.
3 C. J. Burrows and J. G. Muller, *Chem. Rev.*, 1998, **98**, 1109–1152.
4 S. Steenken, *Chem. Rev.*, 1989, **89**, 503–520.
5 (*a*) M. E. Napier and H. H. Thorp, *Langmuir*, 1997, **13**, 6342–6344; (*b*) M. E. Napier, C. R. Loomis, M. F. Sistare, J. Kim, A. E. Eckhardt and H. H. Thorp, *Bioconjugate Chem.*, 1997, **8**, 906–913; (*c*) A. C. Ontko, P. M. Armistead, S. R. Kircus and H. H. Thorp, *Inorg. Chem.*, 1999, **38**, 1842–1846.
6 J. Wang, S. Bollo, J. L. L. Paz, E. Sahlin and B. Mukherjee, *Anal. Chem.*, 1999, **71**, 1910–1913.
7 P. M. Armistead and H. H. Thorp, *Anal. Chem.*, 2000, **72**, 3764–3770.
8 K. M. Millan, A. J. Spurmanis and S. R. Mikkelsen, *Electroanalysis*, 1992, **4**, 929–932.
9 J. Wang, X. Cai, G. Rivas, H. Shiraishi, P. A. M. Farias and N. Dontha, *Anal. Chem.*, 1996, **68**, 2629–2634.
10 H. Kouri-Yousoufi, F. Garnier, P Srivasta and A. Yassar, *J. Am. Chem. Soc.*, 1997, **119**, 7388–7389.
11 T. M. Herne and M. J. Tarlov, *J. Am. Chem. Soc.*, 1997, **119**, 8916–8920.
12 (*a*) T. de Lumley-Woodyear, D. J. Caruana, C. N. Campbell and A. Heller, *Anal. Chem.*, 1999, **71**, 394–398; (*b*) T. de Lumley-Woodyear, C. N. Campbell, E. Freeman, A. Freeman, G. Georgiou and A. Heller, *Anal. Chem.*, 1999, **71**, 535–538.
13 (*a*) E. Palecek, in *Topics in Bioelectrochemistry and Bioenergetics*, ed. G. Milazzo, Wiley, London, 1983, vol. 5, p. 65; (*b*) A. M. Oliveira-Brett and F.-M. Matysik, *Bioelectrochem. Bioenerg.*, 1997, **42**, 111–116; (*c*) A. M. Oliveira-Brett and F.-M. Matysik, *J. Electroanal. Chem.*, 1997, **429**, 95; (*d*) Z. Wang, S. Xiao and Y. Chen, *J. Electroanal. Chem.*, 2006, **589**, 237–242; (*e*) X. Hao, C. Liang and C. Jian-Bin, *Analyst*, 2002, **127**, 834–837.
14 J. Wang, X. Cai, C. Jonsson and M. Balakrishnan, *Electroanalysis*, 1996, **8**, 20–24.
15 J. Wang, J. R. Fernandes and L. T. Kubota, *Anal. Chem.*, 1998, **70**, 3699–3702.
16 P. Singhal, K. T. Kawagoe, C. N. Christian and W. G. Kuhr, *Anal. Chem.*, 1997, **69**, 1662–1668.
17 (*a*) P. Singhal and W. G. Kuhr, *Anal. Chem.*, 1997, **69**, 3552–3557; (*b*) P. Singhal and W. G. Kuhr, *Anal. Chem.*, 1997, **69**, 4828–4832.
18 (*a*) A. Abbaspour and M. A. Mehrgardi, *Anal. Chem.*, 2004, **76**, 5690–5696; (*b*) A. Abbaspour, M. A. Mehrgardi and R. Kia, *J. Electroanal. Chem.*, 2004, **568**, 261–266; (*c*) A. Abbaspour and M. A. Kamyabi, *J. Electroanal. Chem.*, 2005, **576**, 73–83; (*d*) A. Abbaspour, L. Baramakeh and S. M. Nabavizadeh, *Electrochim. Acta*, 2007, **52**, 4798–4803; (*e*) A. Abbaspour and A. Ghaffarinejad, *Electrochim. Acta*, 2008, **53**, 6643–6650.
19 M. V. Rekharsky and Y. Inoue, *Chem. Rev.*, 1998, **98**, 1875–1917.
20 (*a*) K. Birgit, F. Christopher, S. Roswitha, B. Georg and W. Udo, *Anal. Chem.*, 2002, **74**, 3005–3012; (*b*) P. K. Samuel, S. Kimio, K. Toshiyuki, I. Takashi and S. Toshio, *J. Membr. Sci.*, 2004, **230**, 171–174; (*c*) E. M. M. Del Valle, *Proc. Biochem.*, 2004, **39**, 1033–1046.

21 (*a*) A. Ferancová and J. Labuda, *Fresenius' J. Anal. Chem.*, 2001, **370**, 1–10; (*b*) C. A. Nijhuis, B. J. Ravoo, J. Huskens and D. N. Reinhoudt, *Coord. Chem. Rev.*, 2007, **251**, 1761–1780.
22 K. Odashima, M. Kotato, M. Sugawara and Y. Umezawa, *Anal. Chem.*, 1993, **65**, 927–936.
23 Z. Wang, S. Xiao and Y. Chen, *J. Electroanal. Chem.*, 2006, **589**, 237–242.
24 G. Bidan, C. Lopez, F. Mendes-Viegas, E. Vieil and A. Gadelle, *Biosens. Bioelectron.*, 1995, **10**, 219–229.
25 (*a*) H. Kitano, Y. Taira and H. Yamamoto, *Anal. Chem.*, 2000, **72**, 2976–2980; (*b*) Y. Maeda, T. Fukuda, H. Yamamoto and H. Kitano, *Langmuir*, 1997, **13**, 4187–4189; (*c*) H. Kitano and Y. Taira, *Langmuir*, 2002, **18**, 5835–5840; (*d*) H. Kitano, T. Miyamoto and H. Kawasaki, *J. Colloid Interface Sci.*, 2004, **279**, 425–432; (*e*) H. Yamamoto, Y. Maeda and H. Kitano, *J. Phys. Chem. B*, 1997, **101**, 6855–6860; (*f*) H. Endo, T. Nakaji-Hirabayashi, S. Morokoshi, M. Gemmei-Ide and H. Kitano, *Langmuir*, 2005, **21**, 1314–1321; (*g*) T. Fukuda, Y. Maeda and H. Kitano, *Langmuir*, 1999, **15**, 1887–1890.
26 (*a*) L. Z. Zheng, S. G. Wu, X. Q. Lin, L. Nie and L. Rui, *Analyst*, 2001, **126**, 736–738; (*b*) S. Wu, L. Z. Zheng, L. Rui and X. Q. Lin, *Electroanalysis*, 2001, **13**, 967–970; (*c*) L. Z. Zheng, S. G. Wu, X. Q. Lin, L. Nie and L. Rui, *Macromolecules*, 2002, **35**, 6174–6177; (*d*) L. Zheng, S. Wu, X. Q. Lin, C. Shi, L. Nie and L. Rui, *Electroanalysis*, 2003, **15**, 191–195; (*e*) S. Wu and X. Han, *Polym. Degrad. Stab.*, 2005, **90**, 535–539; (*f*) C. Jiang and X. Lin, *J. Power Sources*, 2007, **164**, 49–55.
27 D. Stilwell and S.-M. Park, *J. Electrochem. Soc.*, 1989, **136**, 427–433.
28 F. Hapiot, S. Tilloy and E. Monflier, *Chem. Rev.*, 2006, **106**, 767–781.
29 A. E. Kaifer, *Acc. Chem. Res.*, 1999, **32**, 62–71.
30 (*a*) M. T. Rojas, R. Koniger, J. F. Stoddart and A. E. Kaifer, *J. Am. Chem. Soc.*, 1995, **117**, 336–343; (*b*) C. T. Mallon, R. J. Forster, A. McNally, E. Campagnoli, Z. Pikramenou and T. E Keyes, *Langmuir*, 2007, **23**, 6997–7002.
31 Y-H. Bi, Z-L. Huang and Y-D. Zhao, *Biophys. Chem.*, 2005, **116**, 193–198.
32 (*a*) Y. Wang and A. E. Kaifer, *J. Phys. Chem. B*, 1998, **102**, 9922–9927; (*b*) M. Lahav, K. T. Ranjit, E. Katz and I. Willner, *Chem. Commun.*, 1997, 259–260.
33 (*a*) W. L. Neeley and J. M. Essigmann, *Chem. Res. Toxicol.*, 2006, **19**, 491–505; (*b*) P. G. Slade, M. K. Hailer, B. D. Martin and K. D. Sugden, *Chem. Res. Toxicol.*, 2005, **18**, 1140–1149; (*c*) A. Kupan, A. Saulire, S. Broussy, C. Seguy, G. Pratviel and B. Meunier, *ChemBioChem*, 2006, **7**, 125–133.
34 A. M. Oliveira-Brett, V. Diculescu and J. A. P. Piedade, *Bioelectrochemistry*, 2002, **55**, 61–62.
35 A. J. Bard, L. R. Faulkner, *Electrochemical Methods, Fundamentals and Applications*, Wiley, New York, 2001.
36 (*a*) S. M. Golabi, H. R. Zare and M. Hamzehloo, *Microchem. J.*, 2001, **69**, 111–121; (*b*) A. Salimi and K. Abdi, *Talanta*, 2004, **63**, 475–483.
37 A. M. Oliveira Brett, J. A. P. Piedade and S. H. P. Serrano, *Electroanalysis*, 2000, **12**, 969–973.

